

Updated constraints on decaying cold dark matter

Andreas Nygaard,^a Thomas Tram,^a Steen Hannestad^a

^aDepartment of Physics and Astronomy, Aarhus University, DK-8000 Aarhus C, Denmark

E-mail: andreas@phys.au.dk, thomas.tram@phys.au.dk, steen@phys.au.dk

Abstract. In this paper we update the constraints on the simple decaying cold dark matter (DCDM) model with dark radiation (DR) as decay product. We consider two different regimes of the lifetime, i.e. short-lived and long-lived, and use the most recent CMB data from Planck (2018) to infer new constraints on the decay parameters with which we compare the constraints inferred by the previous Planck data (2015). We hereby show that the newest CMB data constrains the fractional amount of DCDM twice as much as the previous data in the long-lived regime, leading to our current best 2σ upper bound of $f_{\text{dcdm}} < 2.04\%$. In the short-lived regime, we get a slightly looser 2σ upper bound of $f_{\text{dcdm}} < 13.1\%$ compared to the previous CMB data. If we include Baryonic Acoustic Oscillations data from BOSS DR-12, we get an even tighter constraint in the long-lived regime of $f_{\text{dcdm}} < 1.28\%$ and an even looser constraint in the short-lived regime of $f_{\text{dcdm}} < 15.2\%$. We furthermore improve on previous work by thoroughly analysing the impacts of short-lived DCDM on the radiation density and deriving a mapping between short-lived DCDM and a correction, ΔN_{eff} , to the effective number of massless neutrino species.

Contents

1	Introduction	1
1.1	Previous work and constraints	2
1.2	Outline of this paper	3
1.3	Cosmological data	4
2	Boltzmann equations for DCDM and DR	4
2.1	Background equations	4
2.2	Perturbation equations	5
3	Mapping short-lived DCDM to N_{eff}	6
3.1	Analytic solution of Boltzmann equations	6
3.2	Numerical analysis using CLASS	7
4	Current constraints on decay parameters	10
4.1	Long-lived DCDM regime	10
4.2	Short-lived DCDM regime	11
5	Conclusion	15

1 Introduction

Ever since the first inference of the existence of dark matter almost a century ago, the nature of it has remained elusive. Significant progress has been made in establishing its properties. For example it is known that dark matter can only interact weakly with standard model particles (perhaps only through gravitation), and that it must be *cold* in the sense of having sufficiently small thermal velocity so that small scale structure can form. The standard Λ CDM model of cosmology is based on dark matter with exactly these properties and in general provides an excellent fit to observational data.

However, despite many advances in both theory and observations much still remains unknown about the nature of dark matter. For example dark matter could have significant interactions, either with itself or with other particles in a dark sector, separate from the standard model. Such models have been invoked as possible explanations of a variety of anomalies in cosmology, such as the missing satellites problem, the cusp-core problem, and the Hubble tension.

In this paper we investigate the possibility that dark matter is cold and consists of massive particles, but that these particles are unstable and decay. The decay product cannot simply be electromagnetic radiation, since that would be detectable, so instead it is assumed that the decaying cold dark matter (DCDM) decays into massless particles in a dark sector. In line with previous work on the topic we shall refer to the decay product as *dark radiation* (DR), so that we can sketch the process as

$$X_{\text{dcdm}} \rightarrow \gamma_{\text{dr}}.$$

When comparing a model where all dark matter is DCDM with our observational data (Planck, etc.), we need a very large lifetime which renders our DCDM basically stable.

Because of that, we add another degree of freedom to our model which is the initial fraction of DCDM to the total amount of cold dark matter (CDM),

$$f_{\text{dcdm}} = \frac{\Omega_{\text{dcdm}}^{\text{ini}}}{\Omega_{\text{dcdm}}^{\text{ini}} + \Omega_{\text{scdm}}}, \quad (1.1)$$

where SCDM is the stable CDM component. The physical interpretation of having this fractional decay could be [1]:

- 1) CDM is multi-component such that only a part of the dark matter decays,
- 2) all dark matter decays, but the decay product is both dark radiation and a stable CDM component with fraction $(1 - f_{\text{dcdm}})$.

Since the amount of dark matter decreases, we define $\Omega_{\text{dcdm}}^{\text{ini}}$ as the density parameter of DCDM today as if none of it had decayed. We otherwise adopt the same notation as in Ref. [2], which is now standard.

1.1 Previous work and constraints

The field of decaying cold dark matter has been growing ever since the first analysis by Ref. [3] in 2004, where the simple model with dark matter decaying into dark radiation was also used. A lot has happened in the last two decades with the field being much wider now with numerous models of varying sophistication. The different regimes of the decay rate, Γ_{dcdm} , is investigated in Ref. [1] and the fractional amount of DCDM is constrained to $f_{\text{dcdm}} < 3.8 \times 10^{-2}$ using Cosmic Microwave Background (CMB) data from Planck-2015. In this paper we update the results and constraints from Ref. [1] using the newest Planck-2018 data as well as Baryonic Acoustic Oscillations (BAO) data.

It is well known that allowing dark matter to decay can potentially relieve the Hubble tension, and this has been demonstrated numerous times in the literature. This includes Ref. [4] where both the Hubble tension and the milder S_8 tension of matter fluctuations between Λ CDM-model and the model-independent measurements in the local universe were relieved using CMB data from Planck-2018 and the same DCDM model as we are using in this paper. Including other data sets such as BAO data and intermediate-redshift data, however, leads to only a slight decrease in both tensions. Another attempt at relieving the Hubble tension is made in Ref. [5] where the tension is reduced by 1.5σ using Planck-2015 data, BAO data, Redshift Space Distortion (RSD) measurements and a DCDM model with decay time after recombination. By allowing the CMB lensing power amplitude to be a free fitting parameter, the tension is reduced by 3.3σ . They furthermore found an upper limit on the fractional amount of DCDM at the level $f_{\text{dcdm}} \lesssim 5\%$ for DCDM decaying after recombination. The fractional amount of short-lived DCDM is also constrained in Ref. [6] where CMB data from Planck-2015, BAO data, and RSD measurements are used to infer the upper limit $f_{\text{dcdm}} \lesssim 2.73\%$, but this only leads to a slight reduction of the Hubble tension. They furthermore show the impacts of DCDM on the kinetic Sunyaev-Zel'dovich effect and note that this could lead to further constraints on DCDM in the future.

Better and more data has allowed the constraints to be more refined, with different studies using different combinations of data sets. An upper bound on the decay rate of late time DCDM at $\Gamma_{\text{dcdm}} \leq (175 \text{ Gyr})^{-1}$ is inferred in [7] by using CMB data and cluster counts from Planck-2015 along with weak lensing data from KiDS450, while a more tight constraint of $\Gamma_{\text{eff}} < 9.1 \times 10^{-9} \text{ Gyr}^{-1}$ is found in Ref. [8] to the effective decay rate by using Planck-2015

data and analysing cosmic reionisation and dark matter decay simultaneously. A different approach is taken in Ref. [9] where they assume that the decay product is detectable, i.e. a pair production of an elementary particle from the Standard Model (quarks, leptons or bosons), which leads to lower limits on the lifetime in the range $\tau \sim (1 - 5) \times 10^{28}$ s using data from the isotropic gamma-ray background.

There are many studies beyond the simple Λ CDM model, where the decay product is only DR, and a more agnostic approach is found in Ref. [10] where the conversion of dark matter to dark radiation is treated in a more general aspect without assuming the transition being caused by a decay. They then find the impacts of the conversion on the CMB spectrum as well as constraints on their general model parameters using CAMB and COSMOMC, which lead to a reduction in the Hubble tension. They then treat a conversion model in detail where dark matter particles interact via a light mediator particle leading to Sommerfeld-enhanced self-annihilation.

Another, more general analysis is done in Ref. [11] where they investigate Dynamical Dark Matter in which the dark sector is comprised of a large ensemble of particles with different decay widths. Their analysis shows that the constraints allow energy scales ranging from GeV scale to the Planck scale, but the cosmological abundance of the dark sector today must be spread across an increasing number of states in the ensemble as the energy scale is decreased down to GeV scale from the Planck scale. A third continuation of the Λ CDM model is found in Ref. [12] which features Partially Acoustic Dark Matter, where a subdominant part of the dark matter is strongly coupled to the DR fluid, and this combined fluid undergoes acoustic oscillations below the effective dark sound horizon. This is used to reduce the tensions in the Hubble constant and the lensing amplitude between CMB data and direct measurements. They find that even though the model can be used to reduce the tensions separately, it cannot accommodate both at once, since additional CDM is required by the CMB data to preserve the shape of the acoustic peaks.

It has recently been increasingly popular to assume a slightly warm component of the decaying dark matter sector and an analysis of the background equations can be found in Ref. [13] where the cold dark matter decays to both DR and a slightly warm daughter particle. They show that this can potentially relieve the Hubble tension, which makes the model very interesting to future work in the field of cosmology. A slightly different model, where the decaying component is warm and the decay product is only DR, is treated thoroughly in Ref. [14]. The idea of this model is to not modify the evolution of the gravitational potentials, which otherwise leads to inconsistencies with data as in the case of decaying cold dark matter. They find that this can significantly reduce the Hubble tension as well.

1.2 Outline of this paper

In this paper, we are updating the constraints on the Λ CDM model parameters from Ref. [1] using the Markov Chain Monte Carlo (MCMC) sampler MONTE PYTHON [15] and the Einstein–Boltzmann code CLASS [16]. To describe the cosmological framework we will use the following set of parameters:

$$\Theta = \{\Omega_b h^2, \Omega_{\text{cdm}} h^2, h^2, A_s, n_s, \tau_{\text{reio}}\}, \quad (1.2)$$

in addition to the decay parameter vector $\{f_{\text{dcdm}}, \Gamma_{\text{dcdm}}\}$. As was also done in Ref. [1], we will split our MCMC runs into two categories, named *short-lived* and *long-lived*. The reason for this is that the likelihood contour in the full parameter space has a shape which makes convergence exceedingly slow. When the lifetime becomes very short, essentially all Λ CDM

has decayed well before matter-radiation equality. This makes it impossible to constrain Γ_{dcdm} , and the only constrainable quantities are then f_{dcdm} and the product Γf_{dcdm} . This leads to a funnel-like likelihood surface stretching towards very large values of Γ_{dcdm} . This particular part of the parameter space is best probed using a logarithmic prior on Γ_{dcdm} , whereas for the long-lived regime, where only a fraction of the dark matter has decayed before the present, a prior which is flat in Γ_{dcdm} is more suitable. We will elaborate on the technicalities of this split in section 4.

We will furthermore look at an analogous scheme to the short-lived DCDM, i.e. a model with an increase in N_{eff} instead of a decaying dark matter component. This is treated both analytically and numerically using the CLASS code.

The structure of this paper is as follows. We introduce the formal theoretical framework of DCDM in the synchronous gauge in section 2, where both the background equations and the perturbation equations are presented. In section 3 we will treat the mapping between a correction to N_{eff} and short-lived DCDM by deriving an analytical expression for ΔN_{eff} corresponding to a short-lived DCDM component and comparing this to numerical results from CLASS. In section 4 we will present our results from the MCMC sampler MONTE PYTHON along with improved constraints in the long-lived and short-lived regimes, and in section 5 we will conclude and summarize.

1.3 Cosmological data

As our data sets we use the newest CMB data from Planck-2018 [17] which has a higher quality in the polarisation data than its predecessor from 2015 [18]. In all of our computations using Planck-2018, we use both polarisation and temperature likelihoods for both high- ℓ and low- ℓ as well as the lensing likelihood. When comparing to Planck-2015 data, we of course use the corresponding likelihoods from this data release, which is the same combination used in Ref. [1].

We furthermore use the BAO data from BOSS data release 12 (DR-12) [19]. While the BAO data presumably has little impact in parameter constraints in the short-lived regime, due to the decay happening much earlier than the formation of the BAO, it is quite important in the long-lived regime.

2 Boltzmann equations for DCDM and DR

The behaviour of DCDM and DR can be calculated using the Boltzmann equation, which takes the following form for DCDM [1]:

$$\frac{df}{d\tau} = \frac{\partial f}{\partial \tau} + \frac{\partial f}{\partial x^i} \frac{dx^i}{d\tau} + \frac{\partial f}{\partial p} \frac{dp}{d\tau} + \frac{\partial f}{\partial \hat{p}^i} \frac{d\hat{p}^i}{d\tau} = \pm a \Gamma_{\text{dcdm}} f_{\text{dcdm}}, \quad (2.1)$$

with $-$ and $+$ for DCDM and DR respectively.

2.1 Background equations

The zeroth moment of the Boltzmann equation, eq. (2.1), i.e. integrating it over phase-space and keeping only terms of zeroth order, leads to the continuity equation, which is different for DCDM and DR than for the homogeneous universe in having source terms dependent of

the decay rate Γ_{dcdm} with respect to proper time [1]:

$$\begin{aligned}\rho'_{\text{dcdm}} &= -3\frac{a'}{a}\rho_{\text{dcdm}} - a\Gamma_{\text{dcdm}}\rho_{\text{dcdm}}, \\ \rho'_{\text{dr}} &= -4\frac{a'}{a}\rho_{\text{dr}} + a\Gamma_{\text{dcdm}}\rho_{\text{dcdm}},\end{aligned}\tag{2.2}$$

where the prime denotes derivatives with respect to conformal time, τ .

2.2 Perturbation equations

One way of obtaining the relevant perturbation equations is again through the Boltzmann equation, eq. (2.1). We are doing our calculations in the comoving synchronous gauge, so we need to express the perturbation equations in this gauge. Perturbations in the synchronous gauge can be expressed in the following way using the space-time interval [2]:

$$ds^2 = a^2(\tau) \left(-d\tau^2 + [\delta_{ij} + h_{ij}(\mathbf{x}, \tau)] dx^i dx^j \right),\tag{2.3}$$

where the scalar part of the perturbation $h_{ij}(\mathbf{x}, \tau)$ can be expressed through its Fourier transform

$$h_{ij}(\mathbf{x}, \tau) = \int d^3k e^{i\mathbf{k}\cdot\mathbf{x}} \left(h(\mathbf{k}, \tau) \hat{k}_i \hat{k}_j + 6\eta(\mathbf{k}, \tau) \left[\hat{k}_i \hat{k}_j - \frac{1}{3} \delta_{ij} \right] \right),\tag{2.4}$$

with $h(\mathbf{k}, \tau)$ and $\eta(\mathbf{k}, \tau)$ being the metric perturbations in the synchronous gauge. Integrating the Boltzmann equation, eq. (2.1), over phase-space and keeping the first order terms leads to an expression for the evolution of the density perturbation, $\delta_{\text{dcdm}} = \rho_{\text{dcdm}}/\bar{\rho}_{\text{dcdm}} - 1$, where the bar denotes the average value as in a homogeneous universe. We can furthermore find the evolution of the divergence, θ_{dcdm} , of the fluid velocity by taking the divergence of the first moment of eq. (2.1), which is found by multiplying the equation by \vec{p}/E (with \vec{p} and E being the 3-momentum and the energy of a particle respectively) and again integrating over phase-space. The resulting equations are

$$\delta'_{\text{dcdm}} = -\frac{h'}{2},\tag{2.5}$$

$$\theta'_{\text{dcdm}} = -\mathcal{H}\theta_{\text{dcdm}} = 0.\tag{2.6}$$

These two equations are enough to describe the evolution of DCDM since it per definition is cold, which means that we have neglected all second (or higher) order terms of the momentum in our calculations [20]. All higher moments would therefore be zero.

The equations turn out a bit more complicated for DR, since this species is not cold and we therefore cannot neglect higher orders of momentum. Following the same procedure as for DCDM in the synchronous gauge, we get the following equations for the evolution of the density perturbations and the velocity divergence:

$$\delta'_{\text{dr}} = -\frac{2}{3}h' + a\Gamma_{\text{dcdm}} \frac{\rho_{\text{dcdm}}}{\rho_{\text{dr}}} (\delta_{\text{dcdm}} - \delta_{\text{dr}}),\tag{2.7}$$

$$\theta'_{\text{dr}} = \frac{k^2}{4}\delta_{\text{dr}} - k^2\sigma_{\text{dr}} - a\Gamma_{\text{dcdm}} \frac{\rho_{\text{dcdm}}}{\rho_{\text{dr}}}\theta_{\text{dr}}.\tag{2.8}$$

These certainly do not look as simple as those for DCDM, and we notice the parameter σ_{dr} in the bottom equation which is the next moment of the Boltzmann equation - the shear stress.

Generally the evolution of a moment, l , will depend on the next moment, $l + 1$, which leads to an infinite Boltzmann hierarchy for the moments containing the same information as the momentum-dependent Boltzmann equation itself. We still need to truncate the hierarchy at some large l -value to work with it numerically. In the `CLASS` code, the cut-off l -value can be user-specified and is $l_{\text{max}} = 17$ by default.

3 Mapping short-lived DCDM to N_{eff}

In the very short-lived regime, all DCDM has decayed well before matter-radiation equality. In this regime the primary effect of DCDM should be to enhance N_{eff} through the decay product, DR. We define the correction, ΔN_{eff} , as the ratio between the energy densities of the additional radiation (which is DR) and a single massless neutrino. However, we need to evaluate this ratio after the DCDM has fully decayed, where no more DR is produced and the energy density scales as a^{-4} (like any type of radiation),

$$\Delta N_{\text{eff}} = \left. \frac{\rho_{\text{dr}}}{\rho_{\nu}^{N=1}} \right|_{t \gg t_d}, \quad (3.1)$$

where $\rho_{\nu}^{N=1} = 7/8 (4/11)^{4/3} \rho_{\gamma}$ represents only a single massless neutrino [21], and t_d is the time of the decay.

We can estimate how ΔN_{eff} should scale by assuming an instant decay, so the energy density of DR just after the decay equals that of DCDM just before the decay. We can thus evaluate the energy density of DCDM at the time of decay instead of that of DR. We can then scale that to the current time, introducing a_d as the scale factor at the time of decay

$$\Delta N_{\text{eff}} \approx \left. \frac{\rho_{\text{dcdm}}}{\rho_{\nu}^{N=1}} \right|_{t=t_d} \sim a_d \cdot \frac{f_{\text{dcdm}}}{1 - f_{\text{dcdm}}} \cdot \frac{\Omega_{\text{dm},0}}{\Omega_{\nu,0}^{N=1}}. \quad (3.2)$$

Of course this is a very simplistic calculation, but it shows that, as $a_d \rightarrow 0$ (and thus $\Gamma_{\text{dcdm}} \rightarrow \infty$) the effect of DCDM vanishes and the model becomes identical to standard Λ CDM.

3.1 Analytic solution of Boltzmann equations

We can derive an analytic approximation to the Boltzmann equations fairly easily. First, we define

$$Y = a^3 \rho_{\text{dcdm}} / \rho_{\nu,0}, \quad X = a^4 \rho_{\text{dr}} / \rho_{\nu,0}, \quad (3.3)$$

i.e. X and Y are constant in the absence of decays. Here $\rho_{\nu,0}$ is the energy density of all neutrinos today as described by the effective number N_{eff} . The Boltzmann equations (2.2), can then be expressed in proper time as

$$\frac{dY}{dt} = -\Gamma Y(t), \quad \frac{dX}{dt} = a\Gamma Y(t), \quad (3.4)$$

where we have dropped the subscript on the decay rate Γ . The Boltzmann equation for the decaying component then has the solution

$$Y(t) = Y_i e^{-\Gamma t}, \quad (3.5)$$

$$Y_i = a_i^3 \frac{(\rho_{\text{dcdm}})_i}{\rho_{\nu,0}} = \frac{\Omega_{\text{dcdm}}^{\text{ini}}}{\Omega_{\nu,0}} = \frac{\Omega_{\text{dm},0}}{\Omega_{\nu,0}} \cdot \frac{f_{\text{dcdm}}}{1 - f_{\text{dcdm}}}, \quad (3.6)$$

$\Omega_b h^2$	$\Omega_{\text{cdm}} h^2$	h^2	$A_s \times 10^9$	n_s	τ_{reio}	N_{eff}
0.022032	0.11933	0.67556	2.215	0.9619	0.0925	3.046

Table 1: Table of input parameters in CLASS which are held constant through all calculations in section 3.2. N_{eff} is, however, modified with ΔN_{eff} in figure 2.

where the subscript i represents some initial starting point before the decay, and the last equal sign assumes that all DCDM has decayed today, thus making $\Omega_{\text{dm},0}$ both the current density parameter of all dark matter and that of only stable dark matter, since no decaying component is left.

The Boltzmann equation for DR can now be solved using the solution to that of DCDM. We switch coordinates to the scale factor divided by the initial scale factor at the starting point, $\tilde{a} \equiv a/a_i$, and assume that the Universe is radiation dominated throughout the decay so that $a \propto t^{1/2}$. We furthermore define

$$\alpha \equiv \frac{H_i}{\Gamma} = \left(\frac{8\pi G}{3} \rho_{\text{r},0} a_i^{-4} \right)^{1/2} \cdot \frac{1}{\Gamma}, \quad (3.7)$$

where $\alpha \gg 1$. We then integrate the differential equation from the starting point $\tilde{a} = 1$ to find the solution for X (a similar result can be found in Ref. [22])

$$X(a) = X_i + \left[\sqrt{\frac{\pi}{2}} \operatorname{erf} \left(\frac{\tilde{a}}{\sqrt{2\alpha}} \right) - \frac{\tilde{a} e^{-\tilde{a}^2/(2\alpha)}}{\sqrt{\alpha}} \right] \left(\frac{8\pi G}{3} \rho_{\text{r},0} \right)^{1/4} \frac{\Omega_{\text{dm},0}}{\Omega_{\nu,0}} \cdot \frac{f_{\text{dcdm}}}{1 - f_{\text{dcdm}}} \Gamma^{-1/2}, \quad (3.8)$$

where X_i is the initial value of $X(a)$ proportional to the initial DR component (here we have $X_i = 0$ since there is no pre-existing DR component). In the asymptotic limit ($\tilde{a} \rightarrow \infty$) we find

$$X(\tilde{a} \rightarrow \infty) = X_i + \sqrt{\frac{\pi}{2}} \left(\frac{8\pi G \rho_{\text{r},0}}{3} \right)^{1/4} \frac{\Omega_{\text{dm},0}}{\Omega_{\nu,0}} \cdot \frac{f_{\text{dcdm}}}{1 - f_{\text{dcdm}}} \Gamma^{-1/2}, \quad (3.9)$$

and we finally note that $\Delta N_{\text{eff}} = N_{\text{eff}} X(\tilde{a} \rightarrow \infty)$ because of our definition of X . Here we notice the scaling relation $\Delta N_{\text{eff}} \propto \Gamma^{-1/2} f_{\text{dcdm}} / (1 - f_{\text{dcdm}})$. Inserting numbers in eq. (3.9), we arrive at an approximate relation of the form

$$\Delta N_{\text{eff}} \sim 5.74 \Omega_{\text{dm},0} h^2 \frac{f_{\text{dcdm}}}{1 - f_{\text{dcdm}}} \Gamma_6^{-1/2}, \quad (3.10)$$

where $\Gamma_6 = \Gamma / (10^6 \text{Gyr}^{-1})$.

3.2 Numerical analysis using CLASS

Using the CLASS code, we can get an exact numerical correction to N_{eff} caused by short-lived DCDM. The values of input parameters which are held constant in all of the calculations can be seen in table 1 (N_{eff} is modified by ΔN_{eff} in figure 2).

Running CLASS with a high Γ_{dcdm} ($> 10^3 \text{Gyr}^{-1}$) ensures that all DCDM has decayed well before today, which means that the energy density of the resulting DR scales like normal radiation. DR and neutrinos therefore scale similarly, which makes the ratio of their energy densities constant after the decay. This ratio is used to define the correction ΔN_{eff} cf. eq. (3.1). However, because we do not only have a single neutrino, we need to divide the neutrino density with N_{eff} . The numerical value of ΔN_{eff} can in fact be evaluated at any

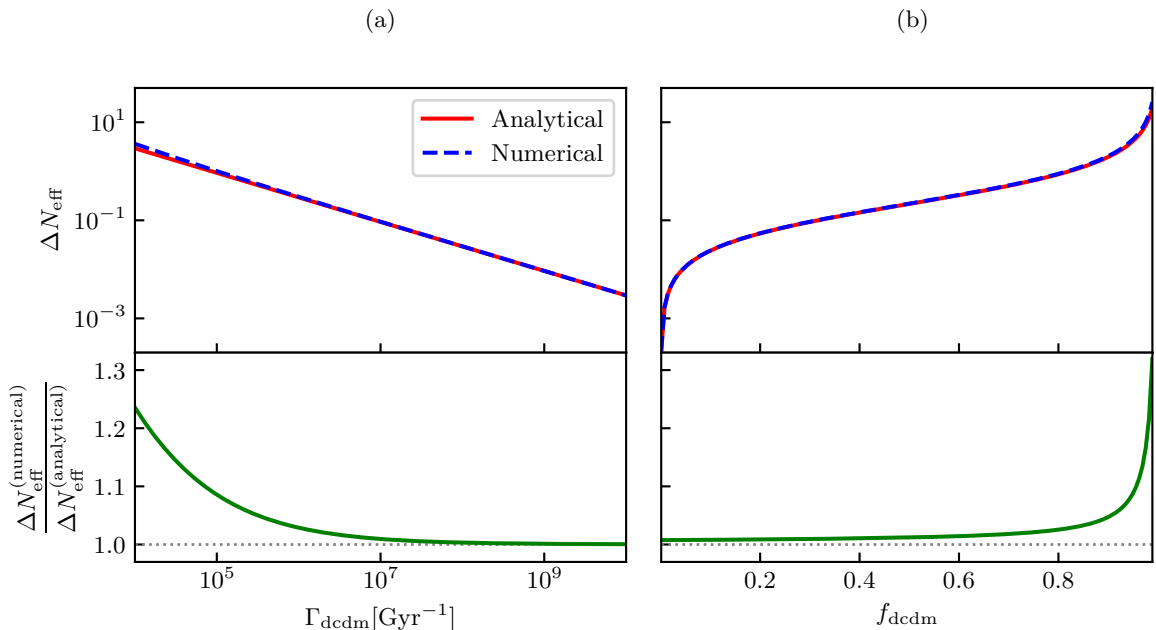


Figure 1: ΔN_{eff} as a function of different parameters for both the numerical result calculated using eq. (3.11) and the analytical result calculated using eq. (3.9). The lower panels show the ratio between the numerical and analytical ΔN_{eff} as a function of the same parameters. The additional parameters used for the simulations are found in table 1. (a) ΔN_{eff} as a function of the decay rate, Γ_{dcdm} , with the fractional amount of DCDM fixed to $f_{\text{dcdm}} = 0.3$. (b) ΔN_{eff} as a function of the fractional amount of DCDM, f_{dcdm} , with the decay rate fixed to $\Gamma_{\text{dcdm}} = 10^7 [\text{Gyr}^{-1}]$.

time after the decay as long as the energy density of DCDM is no longer of any significant size. We, however, evaluate at the current time in order to get a density of DCDM as low as possible,

$$\Delta N_{\text{eff}}^{(\text{numerical})} = N_{\text{eff}} \left. \frac{\rho_{\text{dr}}}{\rho_{\nu}} \right|_{t=t_0}, \quad (3.11)$$

where ρ_{ν} is the total energy density of all massless neutrino species.

At first, we are interested in how well our analytical approach fits the numerical results. Using eq. (3.11), we calculate ΔN_{eff} for different decay rates, Γ_{dcdm} , and fractional amounts of DCDM, f_{dcdm} , and plot the results as functions hereof. This can be seen in the figures 1a and 1b respectively along with the analytical results and the ratio between the two. The numerical and analytical results agree with increasing precision for higher values of Γ_{dcdm} , which is also supported by their ratios approaching unity. Here we also note that both results approach zero for increasing decay rate, which supports that we should recover the Λ CDM model for $\Gamma_{\text{dcdm}} \rightarrow \infty$ as we argued in the beginning of section 3. From figure 1b we, however, see that the analytical and numerical results agree with decreasing precision for higher values of f_{dcdm} , which makes sense according to eq. (3.9) due to the divergence at $f_{\text{dcdm}} = 1$. It should of course behave this way because we cannot have that short-lived DCDM comprises all of the dark matter, since that would correspond to no dark matter at all after recombination, which contradicts some assumptions made in the derivation in section

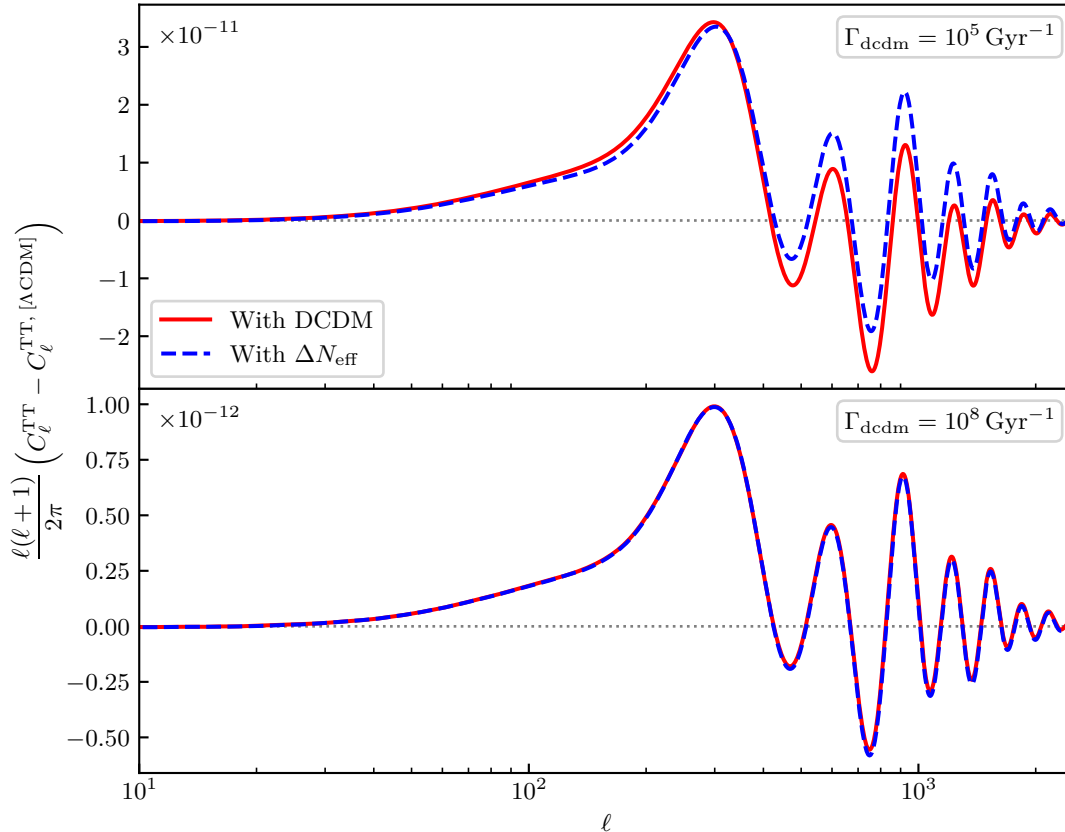


Figure 2: CMB TT power spectra for different values of Γ_{dcdm} and the corresponding $\Delta N_{\text{eff}}^{\text{numerical}}$ (calculated using eq. (3.11)) relative to the power spectrum of the ΛCDM model with no correction to N_{eff} . The additional parameters used for the simulations are found in table 1, and the fractional amount of DCDM is fixed to $f_{\text{dcdm}} = 0.2$.

3.1. Note that the value of ΔN_{eff} also approaches zero for $f_{\text{dcdm}} \rightarrow 0$ which again leads to the ΛCDM model. We also note that the ratio between the analytical and numerical results in figure 1b does not approach unity exactly, but rather a slightly higher value, since the decay rate is fixed at a finite value ($\Gamma_{\text{dcdm}} = 10^7 \text{ Gyr}^{-1}$) and the ratio only approaches unity for $\Gamma_{\text{dcdm}} \rightarrow \infty$, according to figure 1a.

We can now run CLASS again without DCDM, but with the corresponding $\Delta N_{\text{eff}}^{\text{(numerical)}}$ from the DCDM computation instead. According to the theory, we would expect the cosmology of such a run to be similar to that of very short-lived DCDM. Figure 2 shows the CMB TT power spectra of the simulations with DCDM and $\Delta N_{\text{eff}} = \Delta N_{\text{eff}}^{\text{(numerical)}}$ for two values of the decay rate, $\Gamma_{\text{dcdm}} \in \{10^5 \text{ Gyr}^{-1}, 10^8 \text{ Gyr}^{-1}\}$, and a fraction of initial DCDM to all dark matter of $f_{\text{dcdm}} = 0.2$. From this figure it is very clear that the mapping to ΔN_{eff} becomes more accurate for higher values of Γ_{dcdm} , as predicted by the theory. For the lower value of $\Gamma_{\text{dcdm}} = 10^5 \text{ Gyr}^{-1}$, we still see the same behaviour in the power spectra, but they do not overlap as well due to the decay happening much closer to recombination, so a more

significant amount of DR production is still ongoing at the time of the primary CMB signal formation. We also note that the magnitude of the relative power spectra is decreasing for larger Γ_{dcdm} as we would also expect from the theory.

4 Current constraints on decay parameters

In order to obtain constraints on decay parameters we have used the publicly available code MONTE PYTHON [15]. This Markov Chain Monte Carlo (MCMC) sampler uses the Metropolis-Hastings algorithm to sample the probability distribution assuming flat priors. The code is run with four or seven sample chains on a computer cluster until convergence of the chains. Our Gelman-Rubin criterion for convergence of the chains is $R - 1 \lesssim 0.01$, which means that the largest $R - 1$ value of any parameter should be around or smaller than 0.01. The prior of the Γ_{dcdm} parameter is set with different upper and lower bounds depending on which regime we want to analyse. These bounds and the number of sample chains will be stated when necessary.

4.1 Long-lived DCDM regime

The long-lived regime with a decay rate in the interval $\Gamma_{\text{dcdm}} \in [0, 10^3] \text{ Gyr}^{-1}$ corresponds to anything in between the DCDM starting to decay around the time of recombination (and thus having fully decayed by now) and an infinite lifetime where none of the DCDM has decayed yet. The common thing here is that the decay has not finished before recombination which leads to an ongoing DR production after the emission of the CMB. The late decay will thus have an effect on e.g. the angular diameter distance and other background parameters.

Using MONTE PYTHON we search the parameter space with four sample chains using the likelihoods of Planck-2015 and Planck-2018 to see the differences of the two data sets. The result of this is found in figure 3. We have also tried to further constrain the parameters using a combination of Planck-2018 and Baryonic Acoustic Oscillation data (BAO) from BOSS DR12. These results are plotted along with that of only Planck-2018 in figure 4.

From figure 3 we see that the Planck-2018 data constrains the amount of DCDM through the parameter f_{dcdm} much more than the Planck-2015 data does, and our results using Planck-2015 is in great agreement with those found in Ref. [1]. The same is true regarding the constraints on the decay rate, Γ_{dcdm} , which means that the Planck-2018 data favours very long-lived DCDM even more than Planck-2015 data does. The plateau for higher values of Γ_{dcdm} is due to the fact that the data cannot distinguish between the models corresponding to this plateau given that they all imply a very late decay of DCDM (much later than recombination). The plateau continues all the way to the short-lived regime, but we only show the lowest values here. The disagreement in the parameter $\omega_{\text{cdm}}^{\text{ini}} \equiv (\Omega_{\text{dcdm}}^{\text{ini}} + \Omega_{\text{cdm}})h^2$ is mainly due to the disagreement in Ω_{cdm} of the two Planck data sets [17, 18], since the very long-lived DCDM behaves like a stable component and we thus would not expect a significant change to the total dark matter component from that of the Λ CDM model.

In figure 4 we see that the addition of BAO data further constrains the amount of DCDM through f_{dcdm} , and we see a slight change in the posterior of the decay rate as well, lowering the plateau for higher values. The parameter $\omega_{\text{dcdm}}^{\text{ini}}$ seems to be lowered by BAO as well, and this is in agreement with a smaller fractional amount of DCDM being allowed when including BAO, i.e. if f_{dcdm} is smaller, we need a smaller amount of initial dark matter since less is able to decay.

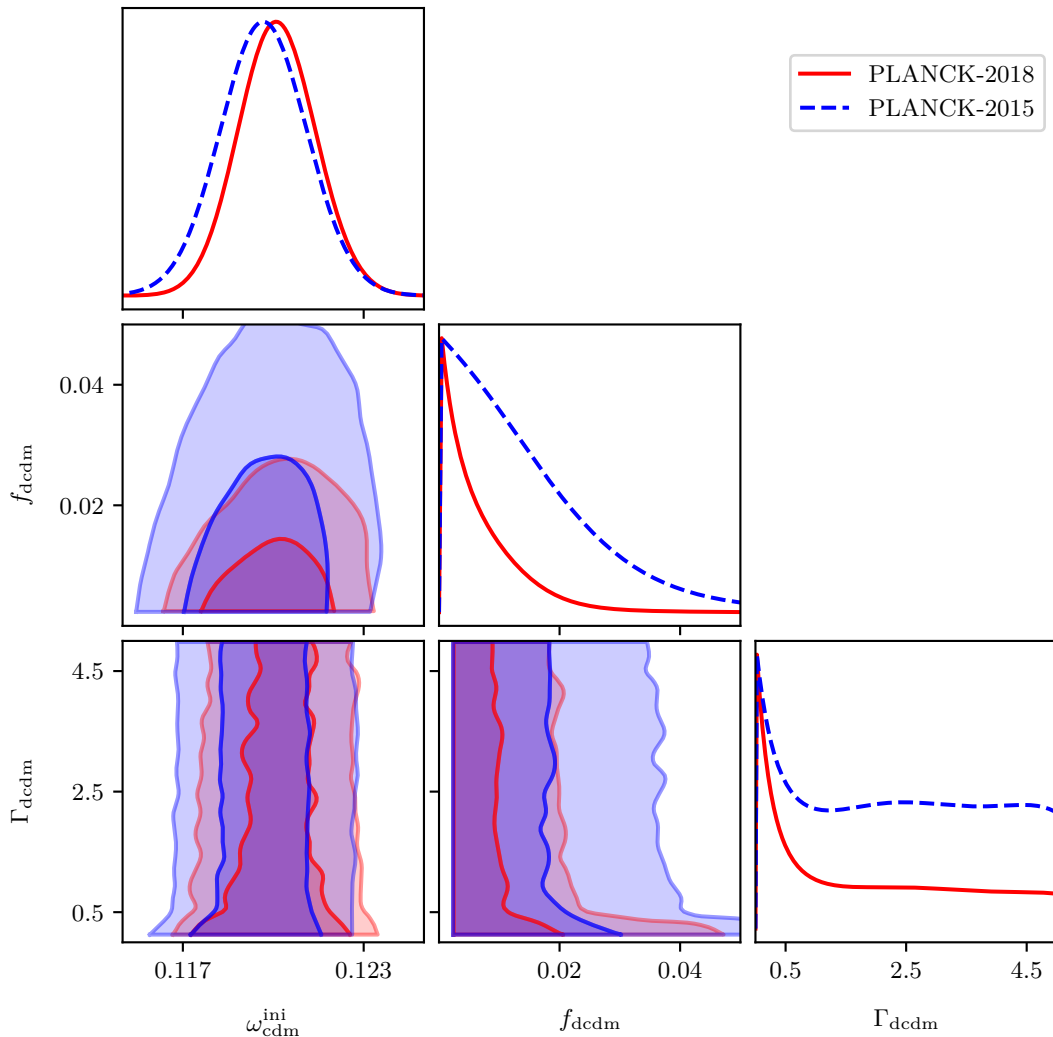


Figure 3: Triangle plot of posteriors in the long-lived regime using the two Planck data sets from 2015 and 2018.

The relevant best fit parameters and constraints in the long-lived regime can be seen in the top panel of table 2 where we see a much tighter constraint on f_{dcdm} inferred by data from Planck-2018 as opposed to data from Planck-2015, and the same is true for the parameter Γf_{dcdm} . We also notice that the inclusion of BAO data further constrains the parameters without changing the bestfit values of H_0 and $\Omega_{\text{cdm}}^{\text{ini}}$.

4.2 Short-lived DCDM regime

In the short-lived regime, the decay rate is rather high ($\Gamma_{\text{dcdm}} > 10^3 [\text{Gyr}^{-1}]$) resulting in most of the DCDM decaying well before recombination. We now search the parameter space using seven sample chains, and in order to search more efficiently, we implement the logarithm

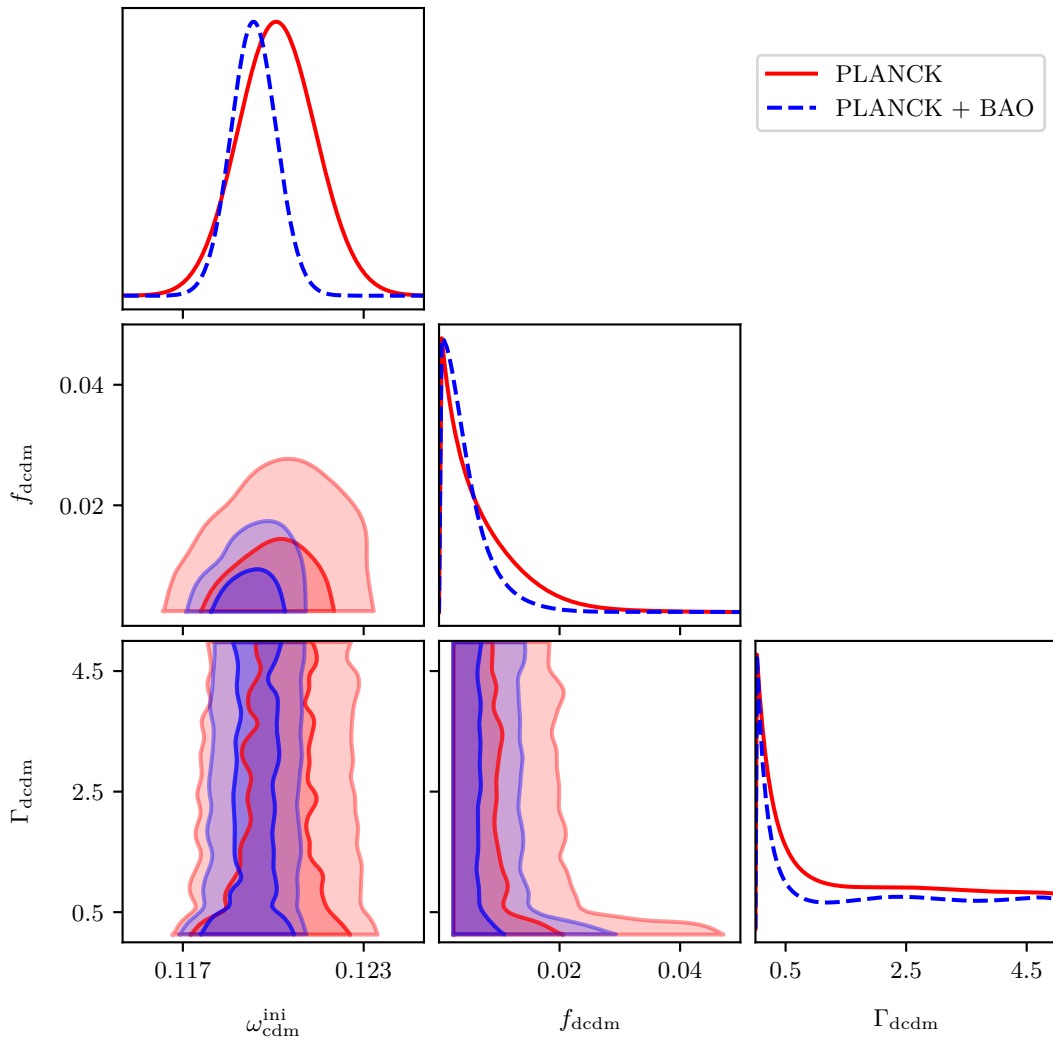


Figure 4: Triangle plot of posteriors in the long-lived regime using Planck-2018 data with and without BAO data from BOSS DR12.

of the decay rate, $\log_{10}(\Gamma_{\text{dcdm}})$, as a parameter in CLASS, which allows us to use this parameter in MONTE PYTHON as well. The parameter space is effectively reduced in size which makes the sampling much faster. We cut the prior at the upper bound $\Gamma_{\text{dcdm}} < 10^6 [\text{Gyr}^{-1}]$ (similar to Ref. [1]) for convergence reasons, but we have checked that the posterior for the decay rate flattens out for increasing values, thus creating another plateau where the data cannot distinguish between the models. To further increase the efficiency we use the flag `-T=2.0` (default 1.0) when running the code, which corresponds to increasing the statistical temperature of the chains so they are more likely to jump further in the parameter space.

The figures 5 and 6 show the posterior distributions in the short-lived regime of Planck-2018 data and either Planck-2015 data or including BAO data respectively. The 1D-posteriors

Long-lived regime	$\Omega_{\text{cdm}}^{\text{ini}} h^2 \times 10^2$	H_0	$f_{\text{dcdm}} \times 10^2$	$\Gamma f_{\text{dcdm}} \times 10^5$
		[$\text{km s}^{-1} \text{Mpc}^{-1}$]		[Gyr^{-1}]
Planck-2015	$12.0^{+0.3}_{-0.3}$	$67.3^{+1.6}_{-1.5}$	< 4.14	< 11.23
Planck-2018	$11.9^{+0.3}_{-0.3}$	$67.7^{+1.2}_{-1.2}$	< 2.04	< 3.54
Planck-2018 + BAO	$11.9^{+0.2}_{-0.2}$	$67.7^{+0.7}_{-0.7}$	< 1.28	< 2.25
Short-lived regime	$\Omega_{\text{cdm}}^{\text{ini}} h^2 \times 10^2$	H_0	$f_{\text{dcdm}} \times 10^1$	$\Gamma f_{\text{dcdm}} \times 10^{-4}$
		[$\text{km s}^{-1} \text{Mpc}^{-1}$]		[Gyr^{-1}]
Planck-2015	$12.6^{+1.5}_{-0.5}$	$67.7^{+1.6}_{-1.6}$	< 0.98	< 2.35
Planck-2018	$12.7^{+1.6}_{-0.8}$	$67.8^{+1.4}_{-1.5}$	< 1.31	< 3.01
Planck-2018 + BAO	$12.5^{+1.8}_{-0.9}$	$68.1^{+1.2}_{-1.3}$	< 1.52	< 3.64

Table 2: Table of parameter constraints in the long-lived and short-lived regimes. We present 2σ constraints corresponding to a 95% confidence level.

of the parameter $\log_{10}(\Gamma_{\text{dcdm}}[\text{Gyr}^{-1}])$ are not shown in their entirety, but rather a closeup of the interesting region is presented by only showing the vertical interval $[0, 0.2]$ (the posteriors are normalised so highest value equals unity).

Figure 5 shows that Planck-2018 data allows for a slightly higher initial dark matter density, $\omega_{\text{cdm}}^{\text{ini}}$, than Planck-2015 data does, which is apparent from the broader peak and longer exponential tail towards higher values in the 1D-posterior. The amount of DCDM allowed by Planck-2018 is also slightly higher which is apparent from the 1D-posterior of f_{dcdm} being slightly broader than that of Planck-2015. The posterior of the decay rate consists of two sub-regimes as explained in Ref. [1], where the small peak (plateau) in the 1D-posterior of Planck-2015 (2018) represents a decay happening mostly in between matter-radiation equality and recombination while the increase in the posterior at larger values of the decay rate represents a decay taking place mostly before matter-radiation equality. Our 1D-posterior of the decay rate for the Planck-2015 data is reminiscent of the one presented in Ref. [1], but with a much less significant peak even though the same data has been used. The difference here could possibly be due to the Gelman-Rubin convergence criterion of the MCMC sampling, where our criterion is an order of magnitude lower than the one used in Ref. [1]. The conclusion, however, does not change by letting the chains converge further, but we do get that the region between the small peak and the subsequent increase is populated more frequently with a stronger convergence criterion, thus diminishing the profoundness of the peak and making it more like a plateau. Using Planck-2018 data we completely transform the peak into a plateau instead.

From figure 6 it is clear that the inclusion of BAO data does not have a significant impact in the short-lived regime, as we previously argued. We see almost the exact same features in the posteriors with the exception that the 1D-posteriors of the initial dark matter density and the fractional amount of DCDM seem broader when including BAO data as opposed to just using Planck-2018 data. This is, however, not significant and we should not draw any conclusions of it, since it could very well be due to our chains not being converged

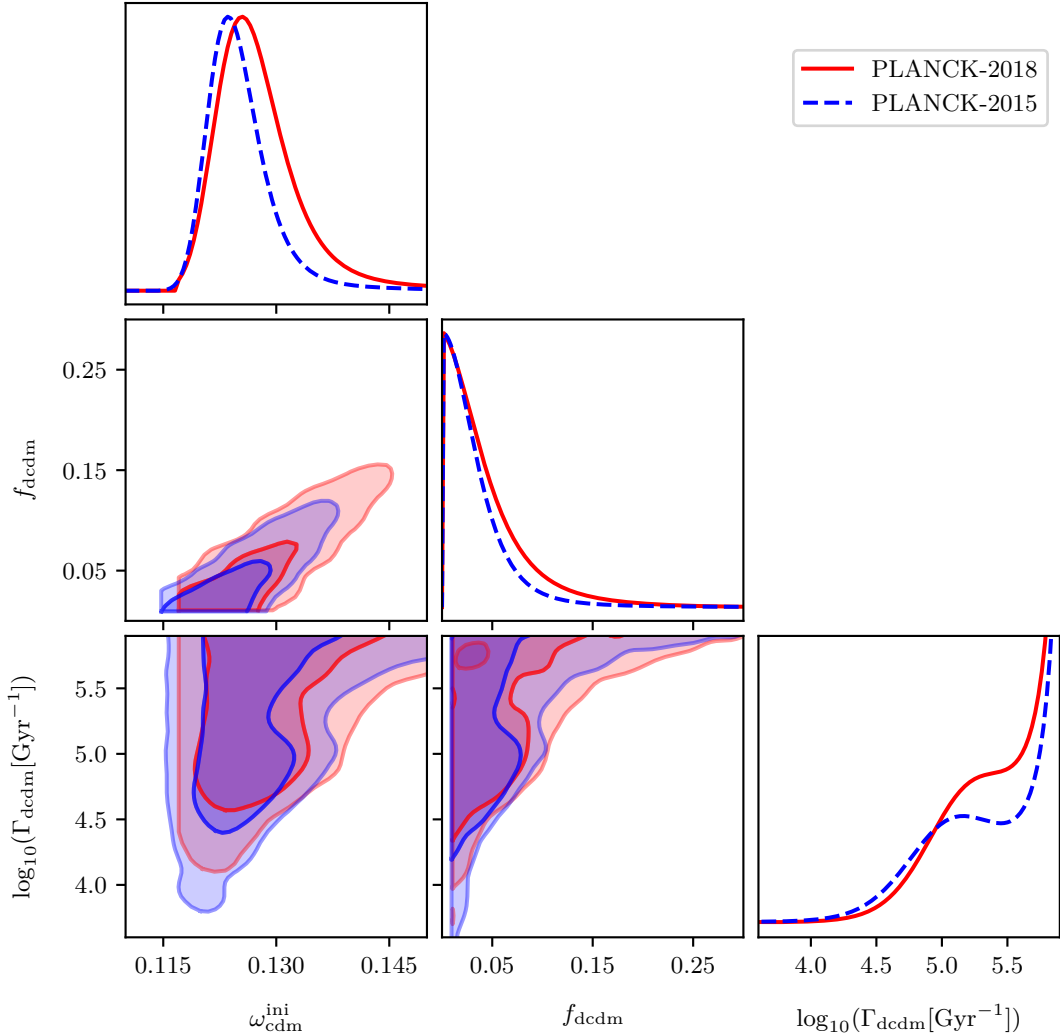


Figure 5: Triangle plot of posteriors in the short-lived regime using the two Planck data sets from 2015 and 2018.

enough. Increasing the amount of sample points or chains could possibly make the difference between the posteriors vanish.

The lower panel of table 2 shows the relevant bestfit values and constraints in the short-lived regime. Here we see more loose constraints of the DCDM parameters from Planck-2018 data than from Planck-2015 data, and even more so when including BAO data. The DCDM parameter constraints do not change as much when including BAO data as in the case of long-lived DCDM, and this agrees with the idea that BAO data only has little impact in short-lived regime.

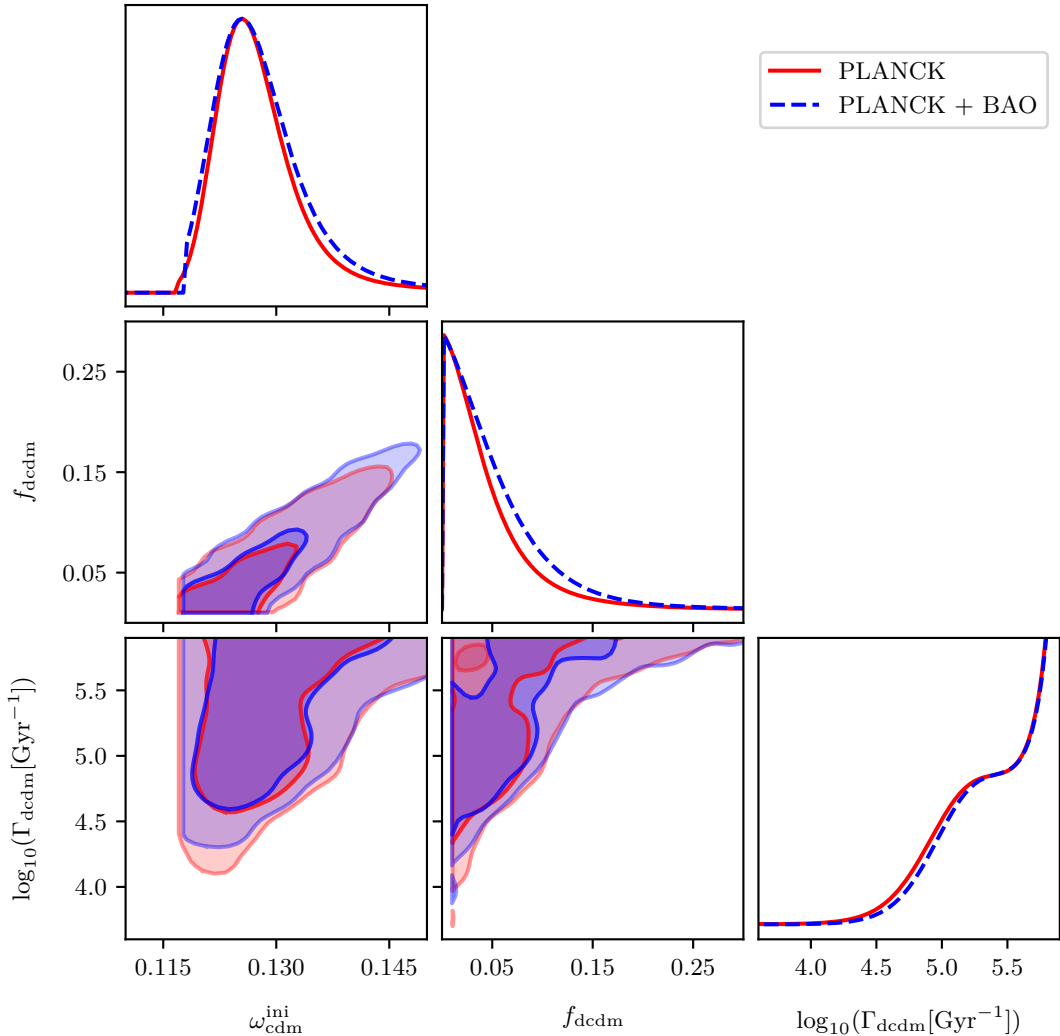


Figure 6: Triangle plot of posteriors in the short-lived regime using Planck-2018 data with and without BAO data from BOSS DR12.

5 Conclusion

Using the MCMC sampler MONTE PYTHON and the most recent CMB data from Planck-2018, we have improved on the previous constraints on the fractional amount of DCDM, f_{dcdm} , as well as the parameter Γf_{dcdm} in the two regimes (long-lived and short-lived). In the long-lived regime, we find that the fractional amount of DCDM is much better constrained by Planck-2018 data (as opposed to Planck-2015 data) leading to an upper bound at 2σ of $f_{\text{dcdm}} < 2.04 \times 10^{-2}$, and the same is true for Γf_{dcdm} for which we find an upper bound at 2σ of $\Gamma f_{\text{dcdm}} < 3.54 \times 10^{-5} \text{Gyr}^{-1}$. These two constraints are tighter than the constraints inferred by Planck-2015 data by factors of ~ 2 and ~ 3 respectively. For the short-lived regime, the Planck-2018 data leads to more loose constraints than Planck-2015 data does, and we

thus find 2σ upper bounds of $f_{\text{dcdm}} < 1.31 \times 10^{-1}$ and $\Gamma f_{\text{dcdm}} < 3.01 \times 10^4 \text{ Gyr}^{-1}$, which are both higher than those of Planck-2015 by a factor of ~ 1.3 .

To further constrain the decay parameters, we have included BAO data from BOSS DR-12 as well. This leads to even tighter constraints in the long-lived regime with 2σ upper bounds of $f_{\text{dcdm}} < 1.28 \times 10^{-2}$ and $\Gamma f_{\text{dcdm}} < 2.25 \times 10^{-5} \text{ Gyr}^{-1}$, while we in the short-lived regime get even looser constraints with 2σ upper bounds of $f_{\text{dcdm}} < 1.52 \times 10^{-1}$ and $\Gamma f_{\text{dcdm}} < 3.64 \times 10^4 \text{ Gyr}^{-1}$.

We have in addition to this investigated how the short-lived DCDM (decaying much earlier than matter-radiation equality) is analogous to a universe without DCDM but with a larger initial amount of non-EM radiation (e.g. massless neutrinos). This has been analytically mapped to a correction to the effective number of massless neutrinos species, N_{eff} , in eq. (3.9). Using the Boltzmann code CLASS we also calculated the actual correction to N_{eff} and saw that this scales in the exact same way as our analytical expression. The analytical and numerical results are also shown to agree with increasing precision as $\Gamma_{\text{dcdm}} \rightarrow \infty$, where we recover the standard Λ CDM model.

Acknowledgements

The numerical results presented in this work were obtained at the Centre for Scientific Computing, Aarhus <http://phys.au.dk/forskning/cscaa/>. A.N. and T.T. was supported by a research grant (29337) from VILLUM FONDEN.

References

- [1] V. Poulin, P. D. Serpico, and J. Lesgourgues, “A fresh look at linear cosmological constraints on a decaying dark matter component,” *JCAP* **08** (2016) 036, [arXiv:1606.02073](#) [[astro-ph.CO](#)].
- [2] C.-P. Ma and E. Bertschinger, “Cosmological perturbation theory in the synchronous and conformal Newtonian gauges,” *Astrophys. J.* **455** (1995) 7–25, [arXiv:astro-ph/9506072](#).
- [3] K. Ichiki, M. Oguri, and K. Takahashi, “WMAP constraints on decaying cold dark matter,” *Phys. Rev. Lett.* **93** (2004) 071302, [arXiv:astro-ph/0403164](#).
- [4] K. L. Pandey, T. Karwal, and S. Das, “Alleviating the H_0 and σ_8 anomalies with a decaying dark matter model,” *JCAP* **07** (2020) 026, [arXiv:1902.10636](#) [[astro-ph.CO](#)].
- [5] A. Chudaykin, D. Gorbunov, and I. Tkachev, “Dark matter component decaying after recombination: Sensitivity to baryon acoustic oscillation and redshift space distortion probes,” *Phys. Rev. D* **97** (2018) no. 8, 083508, [arXiv:1711.06738](#) [[astro-ph.CO](#)].
- [6] L. Xiao, L. Zhang, R. An, C. Feng, and B. Wang, “Fractional Dark Matter decay: cosmological imprints and observational constraints,” *JCAP* **01** (2020) 045, [arXiv:1908.02668](#) [[astro-ph.CO](#)].
- [7] K. Enqvist, S. Nadathur, T. Sekiguchi, and T. Takahashi, “Constraints on decaying dark matter from weak lensing and cluster counts,” *JCAP* **04** (2020) 015, [arXiv:1906.09112](#) [[astro-ph.CO](#)].
- [8] I. M. Oldengott, D. Boriero, and D. J. Schwarz, “Reionization and dark matter decay,” *JCAP* **08** (2016) 054, [arXiv:1605.03928](#) [[astro-ph.CO](#)].
- [9] C. Blanco and D. Hooper, “Constraints on Decaying Dark Matter from the Isotropic Gamma-Ray Background,” *JCAP* **03** (2019) 019, [arXiv:1811.05988](#) [[astro-ph.HE](#)].

- [10] T. Bringmann, F. Kahlhoefer, K. Schmidt-Hoberg, and P. Walia, “Converting nonrelativistic dark matter to radiation,” *Phys. Rev. D* **98** (2018) no. 2, 023543, [arXiv:1803.03644](#) [[astro-ph.CO](#)].
- [11] K. R. Dienes, F. Huang, S. Su, and B. Thomas, “Dynamical Dark Matter from Strongly-Coupled Dark Sectors,” *Phys. Rev. D* **95** (2017) no. 4, 043526, [arXiv:1610.04112](#) [[hep-ph](#)].
- [12] M. Raveri, W. Hu, T. Hoffman, and L.-T. Wang, “Partially Acoustic Dark Matter Cosmology and Cosmological Constraints,” *Phys. Rev. D* **96** (2017) no. 10, 103501, [arXiv:1709.04877](#) [[astro-ph.CO](#)].
- [13] K. Vattis, S. M. Koushiappas, and A. Loeb, “Dark matter decaying in the late Universe can relieve the H0 tension,” *Phys. Rev. D* **99** (2019) no. 12, 121302, [arXiv:1903.06220](#) [[astro-ph.CO](#)].
- [14] N. Blinov, C. Keith, and D. Hooper, “Warm Decaying Dark Matter and the Hubble Tension,” *JCAP* **06** (2020) 005, [arXiv:2004.06114](#) [[astro-ph.CO](#)].
- [15] B. Audren, J. Lesgourgues, K. Benabed, and S. Prunet, “Conservative Constraints on Early Cosmology: an illustration of the Monte Python cosmological parameter inference code,” *JCAP* **1302** (2013) 001, [arXiv:1210.7183](#) [[astro-ph.CO](#)].
- [16] D. Blas, J. Lesgourgues, and T. Tram, “The Cosmic Linear Anisotropy Solving System (CLASS) II: Approximation schemes,” *JCAP* **07** (2011) 034, [arXiv:1104.2933](#) [[astro-ph.CO](#)].
- [17] **Planck** Collaboration, N. Aghanim *et al.*, “Planck 2018 results. VI. Cosmological parameters,” *Astron. Astrophys.* **641** (2020) A6, [arXiv:1807.06209](#) [[astro-ph.CO](#)].
- [18] **Planck** Collaboration, P. Ade *et al.*, “Planck 2015 results. XIII. Cosmological parameters,” *Astron. Astrophys.* **594** (2016) A13, [arXiv:1502.01589](#) [[astro-ph.CO](#)].
- [19] **BOSS** Collaboration, K. S. Dawson *et al.*, “The Baryon Oscillation Spectroscopic Survey of SDSS-III,” *Astron. J.* **145** (2013) 10, [arXiv:1208.0022](#) [[astro-ph.CO](#)].
- [20] S. Dodelson, *Modern Cosmology*. Academic Press, Amsterdam, 2003.
- [21] **Particle Data Group** Collaboration, M. Tanabashi *et al.*, “Review of Particle Physics,” *Phys. Rev. D* **98** (2018) no. 3, 030001.
- [22] R. J. Scherrer and M. S. Turner, “Decaying Particles Do Not Heat Up the Universe,” *Phys. Rev. D* **31** (1985) 681.